Journal of Engineering Physics and Thermophysics, Vol. 80, No. 2, 2007

INFLUENCE OF PHASE TRANSFORMATIONS AND HEAT AND MASS EXCHANGE ON THE COURSE OF THE PROCESSES OF PYROLYSIS OF SINGLE HIGH-ASH-COAL PARTICLES AT ELEVATED PRESSURES

V. P. Patskov

UDC 662.61.747:66.096.5

A comparative analysis of equilibrium and nonequilibrium models for calculation of the rates of phase transitions (evaporation and condensation) of pyrolysis products and the influence of convective heat and mass exchange with inert ash particles and the gas flow in pyrolysis of single particles of high-ash coals in the operation of technological units with a circulating fluidized bed under pressure is made.

Introduction. Thermal pretreatment of fuel in external (detachable) pyrolysis apparatuses at elevated pressures and high-rate heating is one important step of the processes of thermochemical processing (pyrolysis, burning, and gasification) of high-ash power-generating coals in technological units with different fluidized-bed modifications [1, 2].

The process of thermal decomposition of coals in heating in an inert, oxidizing, or gasification medium is a complex process of irreversible physicochemical transformations resulting in the formation of solid, liquid, and gaseous products from the initial solid fuel [3]. The yield and composition of these products are determined by the distinctive features of the molecular structure and by heating conditions. The process of decomposition of coals at atmospheric pressure, in slow heating, and with forced evacuation of gaseous products by an inert carrier gas, i.e., the basis of carbonization or low-temperature-carbonization technologies, is most completely understood [4, 5]. Experimental data on the dynamics and macrokinetics of high-rate pyrolysis of high-ash power-generating coals are extremely limited [3, 6] as are the correct mathematical models of these processes [7–13]. Such is the case for experimental data under pressure or for a limited rate of evacuation of products [3, 14–16]. This is because of the very complex and multistage chemical transformations in the pyrolysis of solid fuels [4, 5, 17] with various and virtually unknown compositions of the resins released [17], of the substantial influence of physical stages (effective diffusion, heat conduction, convective-filtration transfer, and phase transitions) [5, 7–13, 18, 19] and secondary heterogeneous reactions of interaction of the pyrolysis products with the carbon-ash residue of the fuel [13, 18, 19] on the course of the process, and of the presence of three interacting phases — the organic mineral skeleton (carbon-ash fuel residue, moisture, volatiles, and ash) and the gaseous (products of pyrolysis and chemical transformations) and intermediate condensed phases (resins and hydrocarbons, dissolved and condensed gases) — in the pores.

Calculation of the rates of phase transitions (evaporation and condensation) of resins and hydrocarbons and release of condensed and dissolved gases from the liquid phase to a gas phase in the pores represents a special problem [18, 19]. Also, an analysis of the processes of thermocontact pyrolysis of high-ash coals at elevated pressures, when they are heated by convective and radiative heat exchange from inert ash particles added to the fuel bed for stabilizing the temperature regime, is a challenge [20]. Information available in the literature is devoted mainly to studying either the external heat and mass exchange in the bed (surface–bed) [21] or the internal (particle–gas) exchange under conditions where all particles are active [7–13, 18, 19]. Systems intermediate between these two limiting cases, among which are the pyrolysis processes in question, have so far been studied only partially [21, 22].

The present work seeks to numerically model the process of thermocontact pyrolysis of a single particle of high-ash bituminous coal under conditions where the thermodynamic equilibrium between the concentrations of the

---

Institute of Coal Power Technologies, National Academy of Sciences and Ministry of Fuel and Power of Ukraine, 19 Andreevskaya Str., Kiev, 04070, Ukraine; email: vadimpatskov1@rambler.ru. Translated from Inzhenerno-Fizicheskii Zhurnal, Vol. 80, No. 2, pp. 127–138, March–April, 2007. Original article submitted July 20, 2005; revision submitted September 12, 2006.

components in condensed and gas phases in the pores is upset (the process of phase transitions is nonequilibrium). The particle is in a fluidized bed; it is covered with a gas blanket and is surrounded by inert ash particles.

An analysis is carried out on the basis of the equilibrium mathematical model proposed earlier [11–13, 18, 19]. The model assumes the presence of the three phases mentioned above within the porous structure of a spherical coal particle. The gaseous phase contains the vapor of resins and hydrocarbons, CO_2, CO, H_2O, H_2, CH_4, C_2H_4, C_2H_6, and N_2. The resin consists of seven key components that reflect the basic structures forming part of the coal molecule [17]: benzene C_6H_6, toluene C_7H_8, phenol C_6H_5OH, dimethylnaphthalene $C_{11}H_{24}$, undecane $C_{12}H_{12}$, methyl ethyl tetralin $C_{13}H_{18}$, and phenanthrene $C_{14}H_{10}$. We allow for the effective diffusion, heat conduction, convective-filtration transfer by Darcy's law in the gas and condensed phases, convective transfer in the condensed phase due to the capillary diffusion and different viscosities of the components of the resin and degrees of wettability of the fuel pores [23–25], secondary heterogeneous reactions of gasification of the carbon-ash fuel residue, and phase transitions of the components of the intermediate condensed phase. We take the temperatures of the phases in the pores to be equal and the stages of primary moisture and volatile yield to be fast [6, 11–13]. Furthermore, we allow for the accepted propositions of multiphase hydrodynamics [24]: a spherical particle shape, the homogeneity of each phase, and the possibility of averaging the parameters over volume elements.

In accordance with the assumptions made above, the mathematical model of the process of thermocontact pyrolysis of a single high-ash-coal particle has the form [18, 19]

$$\frac{\partial}{\partial t}\left[\alpha_1\rho_1 C_{1j}\right]=\frac{1}{r^2}\frac{\partial}{\partial r}\left[D_{1j}^{\mathrm{eff}}\alpha_1\rho_1 r^2\frac{\partial C_{1j}}{\partial r}\right]-\frac{1}{r^2}\frac{\partial}{\partial r}\left[u_1\alpha_1\rho_1 C_{1j}r^2\right]+\overline{W}_{\mathrm{ph.tr}}C_{1j}^{\mathrm{eq}}+$$

$$+\overline{q}_{\mathrm{vol}j}+\overline{q}_{\mathrm{w}}\pm\sum_{s=1}^{N_s}\nu_{s,j}W_s\alpha_2F_{\mathrm{sp}}\,,\quad j=\overline{1,m_{\mathrm{gas}}}\,; \tag{1}$$

$$\frac{\partial}{\partial t}\left[\alpha_1\rho_1\right]=-\frac{1}{r^2}\frac{\partial}{\partial r}\left[u_1\alpha_1\rho_1 r^2\right]+\overline{W}_{\mathrm{ph.tr}}\sum_{j=1}^{m_{\mathrm{liq}}}C_{1j}^{\mathrm{eq}}+\overline{q}_{\mathrm{w}}+\sum_{j=1}^{m_{\mathrm{vol}}}\overline{q}_{\mathrm{vol}j}+\sum_{s=1}^{N_s}\nu_{sc}W_s\alpha_2F_{\mathrm{sp}}\,; \tag{2}$$

$$\frac{\partial}{\partial t}\left[\alpha_2\rho_2 C_{2j}\right]=-\overline{\Phi}_{s,j}\,,\quad j=\overline{1,m_{\mathrm{sol}}}\,; \tag{3}$$

$$\frac{\partial}{\partial t}\left[\alpha_2\rho_2\right]=-\sum_{s=1}^{N_s}\nu_{sc}W_s\alpha_2F_{\mathrm{sp}}-\sum_{j=1}^{m_{\mathrm{vol}}}\overline{q}_{\mathrm{vol}j}-\overline{q}_{\mathrm{w}}\,; \tag{4}$$

$$\frac{\partial}{\partial t}\left[\alpha_3\rho_3 C_{3j}\right]=\frac{1}{r^2}\frac{\partial}{\partial r}\left[D_{3j}^{\mathrm{eff}}\alpha_3\rho_3 r^2\frac{\partial C_{3j}}{\partial r}\right]-\frac{1}{r^2}\frac{\partial}{\partial r}\left[u_3\alpha_3\rho_3 r^2 C_{3j}\right]-\overline{W}_{\mathrm{ph.tr}}C_{1j}^{\mathrm{eq}}\,,\quad j=\overline{1,m_{\mathrm{liq}}}\,; \tag{5}$$

$$\frac{\partial}{\partial t}\left[\alpha_3\rho_3\right]=-\frac{1}{r^2}\frac{\partial}{\partial r}\left[u_3\alpha_3\rho_3 r^2\right]-\overline{W}_{\mathrm{ph.tr}}\,; \tag{6}$$

$$\frac{\partial}{\partial t}\left[c_p^{\mathrm{eff}}T_{\mathrm{p}}\right]=\frac{1}{r^2}\frac{\partial}{\partial r}\left[\lambda_{\mathrm{p}}^{\mathrm{eff}}r^2T_{\mathrm{p}}\right]-\frac{1}{r^2}\frac{\partial}{\partial r}\left[T_{\mathrm{p}}r^2\left(u_1\alpha_1\rho_1c_{p1}+u_3\alpha_3\rho_3c_{p3}\right)\right]+$$

$$+ \overline{W}_{\mathrm{ph.tr}} \, \Delta H_{\mathrm{ph.tr}} - \bar{q}_{\mathrm{w}} \Delta H_{\mathrm{w}} + \sum_{s=1}^{N_s} W_s Q_s \alpha_2 F_{\mathrm{sp}} \, ; \tag{7}$$

$$\sum_{j=1}^{m_{\mathrm{gas}}} C_{1j} = \sum_{j=1}^{m_{\mathrm{sol}}} C_{2j} = \sum_{j=1}^{m_{\mathrm{liq}}} C_{3j} = \sum_{i=1}^{3} \alpha_i = 1 \, ; \tag{8}$$

$$P_1 = RT_{\mathrm{p}} \rho_1 \sum_{j=1}^{m_{\mathrm{gas}}} \frac{C_{1j}}{M_j} \, ; \quad \rho_2 = f_2 \, (C_{2j}) \, ; \quad \rho_3 = f_3 \, (C_{3j}) \, ; \tag{9}$$

$$t = 0 : \quad C_{1j} = C_{1j}^{0} \quad (j = 1, ..., m_{\mathrm{gas}}) \, ; \quad C_{2j} = C_{2j}^{0} \quad (j = 1, ..., m_{\mathrm{sol}}) \, ; \quad C_{3j} = 0 \quad (j = 1, ..., m_{\mathrm{liq}}) \, ;$$

$$\rho_i = \rho_i^0 \quad (i = 1, 2, 3) \, ; \quad P_1 = P_1^0 \, ; \quad T_{\mathrm{p}} = T_{\mathrm{p}}^0 \, ; \quad \alpha_3 = \alpha_3^0 \, ; \quad \alpha_1 = \varepsilon_0 \, ; \tag{10}$$

$$r = 0 : \quad \frac{\partial C_{1j}}{\partial r} = \frac{\partial C_{3j}}{\partial r} = \frac{\partial \alpha_3}{\partial r} = \frac{\partial P_1}{\partial r} = \frac{\partial T_{\mathrm{p}}}{\partial r} = 0 \, ; \tag{11}$$

$$r = r_{\mathrm{p}} : \quad D_{1j}^{\mathrm{eff}} \alpha_1 \rho_1 \frac{\partial C_{1j}}{\partial r} - u_1 \alpha_1 \rho_1 C_{1j} + \left(\overline{W}_{\mathrm{ph.tr}} C_{1j}^{\mathrm{eq}} + \bar{q}_{\mathrm{vol}j} + \bar{q}_{\mathrm{w}} + \sum_{s=1}^{N_s} \nu_{s,j} W_s \right) \Big/ F_{\mathrm{sp}} =$$

$$= \beta_j \left(\rho_{1j}^0 - \rho_{1j} \right), \quad j = \overline{1, m_{\mathrm{gas}}} \, ; \tag{12}$$

$$C_{3j} = 0 \quad (j = 1, ..., m_{\mathrm{liq}}) \, ; \quad \alpha_3 = 0 \, ; \quad \rho_3 = \rho_3^0 \, ; \tag{13}$$

$$\lambda_{\mathrm{p}}^{\mathrm{eff}} \frac{\partial T_{\mathrm{p}}}{\partial r} - u_1 \alpha_1 \rho_1 c_{p1} T_{\mathrm{p}} - u_3 \alpha_3 \rho_3 c_{p3} T_{\mathrm{p}} + c_{p1} T_{\mathrm{p}} \sum_{j=1}^{m_{\mathrm{gas}}} D_{1j}^{\mathrm{eff}} \alpha_1 \rho_1 \frac{\partial C_{1j}}{\partial r} + c_{p3} T_{\mathrm{p}} \sum_{j=1}^{m_{\mathrm{liq}}} D_{3j}^{\mathrm{eff}} \alpha_3 \rho_3 \frac{\partial C_{3j}}{\partial r} +$$

$$+ \left(\sum_{s=1}^{N_s} W_s Q_s - \overline{W}_{\mathrm{ph.tr}} \, \Delta H_{\mathrm{ph.tr}} - \bar{q}_{\mathrm{w}} \Delta H_{\mathrm{w}} \right) \Big/ F_{\mathrm{sp}} = H_{\mathrm{conv}}^{*} \left(T^{*} - T_{\mathrm{p}} \right) + \varepsilon_{\mathrm{c}}^{*} \sigma_0 \left[\left(\frac{T^{*}}{100} \right)^4 - \left(\frac{T_{\mathrm{p}}}{100} \right)^4 \right] . \tag{14}$$

The density of the intermediate condensed phase and the coefficients of effective diffusion in it are determined on the basis of recommendations [26]. The rate of convective-filtration transfer in this phase is calculated based on the equation [23–25]

$$u_3 = - \gamma_3 \frac{\partial P_1}{\partial r} \pm \mathrm{B} \, \frac{\partial \alpha_3}{\partial r} \, , \tag{15}$$

where the permeability coefficient is determined from the formula [23–25, 27]

$$\gamma_3 = \frac{\alpha_3}{8\tau\mu_3}(r_l)^2 ,$$

and the radius of flooded pores is calculated from the expression [27]

$$r_l = \frac{\int\limits_{r_{\min}}^{r_{\rm cr}} r f(r)\, dr}{\int\limits_{r_{\min}}^{r_{\rm cr}} f(r)\, dr} . \tag{16}$$

The minimum pore radius in expression (16) is determined in accordance with the pore-size distribution function [27]:

$$f(r) = \frac{r \exp\left(-\frac{r}{\bar{r}}\right)}{(\bar{r})^2} . \tag{17}$$

The differential equation for evaluation of the critical dimension $r_{\rm cr}$ follows from Darcy's law for the condensed phase (15) and from the equation for evaluation of the capillary pressure [27]:

$$\frac{dr_{\rm cr}}{dr} = \frac{u_3 + \gamma_3 \frac{\partial P_1}{\partial r}}{\frac{2\gamma_3 \sigma \cos\varphi}{[r_{\rm cr}]^2}} .$$

The capillary-soaking parameter B in Eq. (15) is dependent on the pore structure in a more complex manner [23–25]:

$$\mathrm{B} = \frac{2\sigma\cos\varphi}{b_0\mu_3} \frac{\sum\limits_{l=1}^{L} r_l^2 \frac{dr_l}{d\alpha_3}}{\sum\limits_{l=1}^{L} r_l^3} = \frac{1}{b_0\mu_3} \frac{\sum\limits_{l=1}^{L} r_l^4 \frac{dP_{\rm cap}}{d\alpha_3}}{\sum\limits_{l=1}^{L} r_l^2} . \tag{18}$$

Just as γ_3, the parameter B is determined, on the one hand, by the maximum radius of flooded pores, and, on the other hand, by the distribution of the flooded pores on the particle radius. Also, expression (18) involves the derivative $dP_{\rm cap}/d\alpha_3$ dependent on the direction of motion of the intermediate condensed phase (on whether we have impregnation of the particle pores with resin or its drainage). A hysteresis may be observed in the dependence of the capillary pressure on the fraction of the intermediate condensed phase. Also, characteristically the displacement of the liquid by the gas occurs only when the pressure in the latter becomes higher than a certain breakdown pressure $P_{\rm br}$ and is observed to a certain residual value of $\alpha_3^{\rm res}$. The connectivity of the liquid phase disappears. Analogously the particle is impregnated with liquid until a certain residual value of the gas content $\alpha_1^{\rm res}$ is attained. The presence of the hysteresis and such a complex dependence of the capillary pressure on α_3 makes it noticeably more difficult to calculate the rate of convective-filtration transfer in the intermediate condensed phase.

Unlike the equilibrium model [18, 19], the total rate of phase transition $\overline{W}_{\rm ph.tr}$ under nonequilibrium conditions may be evaluated based on the following approach [23, 25]. Thus, according to an analysis of the equations of continuity of flows in the gas (2) and intermediate (6) condensed phases, the relation

$$-\overline{W}_{\mathrm{ph.tr}} = -\overline{W}_{\mathrm{ph.tr}} \sum_{j=1}^{m_{\mathrm{liq}}} C_{1j}^{\mathrm{eq}} + \bar{q}_{\mathrm{w}} + \sum_{j=1}^{m_{\mathrm{vol}}} \bar{q}_{\mathrm{vol}j} + \sum_{s=1}^{N_s} \nu_{sc} W_s \alpha_2 F_{\mathrm{sp}} \tag{19}$$

must hold. From (19), we find that the total phase-transition rate caused by the dissolution of gaseous components in the resin and by the evaporation and condensation of resins and hydrocarbons is equal to

$$\overline{W}_{\mathrm{ph.tr}} = -\frac{\bar{q}_{\mathrm{w}} + \sum\limits_{j=1}^{m_{\mathrm{vol}}} \bar{q}_{\mathrm{vol}j} + \sum\limits_{s=1}^{N_s} \nu_{sc} W_s \alpha_2 F_{\mathrm{sp}}}{1 - \sum\limits_{j=1}^{m_{\mathrm{liq}}} C_{1j}^{\mathrm{eq}}} . \tag{20}$$

In (20), the rate of release of the primary adsorbed moisture from the particle pores may be determined from the dependence [6]

$$\bar{q}_{\mathrm{w}} = -\frac{dC_{2,3}}{dt} = k_{\mathrm{w}}^0 \exp\left[\frac{E_{\mathrm{w}}}{R}\left(\frac{1}{T_{\mathrm{p}}^0} - \frac{1}{T_{\mathrm{p}}}\right)\right]\left(1 - \frac{C_{2,3}}{W^{\mathrm{work}}}\right)^{n_{\mathrm{w}}} . \tag{21}$$

The rates of primary release of volatiles in (20) are determined in accordance with [5, 6, 11, 12]

$$\bar{q}_{\mathrm{vol}j} = -\frac{dC_{2j}}{dt} = k_{\mathrm{vol}j}^0 \exp\left[\frac{E_{\mathrm{vol}j}}{R}\left(\frac{1}{T_{\mathrm{p}}^0} - \frac{1}{T_{\mathrm{p}}}\right)\right]\left(1 - \frac{C_{2j}}{V^{\mathrm{work}}}\right)^{n_{\mathrm{vol}j}} , \quad j = \overline{1, m_{\mathrm{vol}}} . \tag{22}$$

Expression (20) also involves the rates of heterogeneous interaction of the carbon-ash residue of the fuel with the CO_2, H_2O, and H_2 pyrolysis products. The rate of gasification of coke with CO_2 is determined on the basis of the dependence [28]

$$W_1 = \frac{k_1^0 \exp\left[\frac{E_1}{R}\left(\frac{1}{T_{\mathrm{p}}^0} - \frac{1}{T_{\mathrm{p}}}\right)\right] p_{\mathrm{CO_2}}}{1 + k_2^0 \exp\left[\frac{E_2}{R}\left(\frac{1}{T_{\mathrm{p}}} - \frac{1}{T_{\mathrm{p}}^0}\right)\right] p_{\mathrm{CO_2}} + k_3^0 \exp\left[\frac{E_3}{R}\left(\frac{1}{T_{\mathrm{p}}} - \frac{1}{T_{\mathrm{p}}^0}\right)\right] p_{\mathrm{CO}}} . \tag{23}$$

The reaction of vapor gasification of the carbon-ash residue in (20) is calculated analogously [29]:

$$W_2 = \frac{k_4^0 \exp\left[E_4^*\left(\frac{1}{T_{\mathrm{p}}^0} - \frac{1}{T_{\mathrm{p}}}\right)\right] p_{\mathrm{H_2O}}}{1 + k_5^0 \exp\left[E_5^*\left(\frac{1}{T_{\mathrm{p}}} - \frac{1}{T_{\mathrm{p}}^0}\right)\right] p_{\mathrm{H_2O}} + k_6^0 \exp\left[E_6^*\left(\frac{1}{T_{\mathrm{p}}} - \frac{1}{T_{\mathrm{p}}^0}\right)\right] p_{\mathrm{H_2}}} . \tag{24}$$

Finally, the reaction rate of hydrogasification of the fuel is evaluated in accordance with the Arrhenius dependence of first order [29]

$$W_3 = k_7^0 \exp\left[E_7^* \left(1/T_{\mathrm{p}}^0 - 1/T_{\mathrm{p}}\right)\right] p_{\mathrm{H_2}} . \tag{25}$$

In formulas (24) and (25), we have $E_i^* = E_i/R$. The equilibrium concentrations in Eq. (20) are determined from the combined Raoult–Dalton law [23–27, 30, 31]

$$y_{1j}^{\mathrm{p}} = C_{3j}^* \left(p_{1j}^0/P_1\right) \exp\,[\{-\left(2\sigma V_j^{\mathrm{m}} \cos\varphi/RT_{\mathrm{p}} r_{\mathrm{cr}}\}\right] \,, \quad j = 1, \ldots, m_{\mathrm{vol}} \,. \tag{26}$$

In formula (26), the partial pressures of the jth gaseous component as functions of the particle temperature are computed from the approximation polynomials [30], whereas the specific mole volumes of the components are calculated according to the recommendations of [31].

The effective heat capacity and thermal conductivity of the particle are found as additive quantities from the formulas [23, 25, 27]

$$c_p^{\mathrm{eff}} = \sum_{i=1}^{3} \alpha_i \rho_i c_{pi} \,, \quad \lambda_p^{\mathrm{eff}} = \sum_{i=1}^{3} \alpha_i \lambda_i \,.$$

The heat capacities and thermal conductivities of the components and the phases are determined in accordance with the recommendations of [30, 32, 33]. The rate of convective-filtration transfer in the gaseous phase is found from Darcy's law [8–13, 18, 19, 23–25, 27]

$$u_1 = -\gamma_1 \partial P_1/\partial r \,, \tag{27}$$

where $\gamma_1 = \alpha_1 (r_{\mathrm{g}})^2/8\tau$ is the coefficient of permeability in the gaseous phase [23, 25, 27], r_{g} is the radius of gas-filled pores:

$$r_{\mathrm{g}} = \frac{\int_{r_{\mathrm{cr}}}^{r_{\max}} r f(r)\, dr}{\int_{r_{\mathrm{cr}}}^{r_{\max}} f(r)\, dr}$$

($r_{\max}$ is the maximum pore radius determined from the pore-size distribution function (16)).

The effective coefficients of diffusion in the gas phase are evaluated by the recommendations of [25, 27, 34], the heats of evaporation of the components of the intermediate phase and moisture are determined from [30], the thermal reaction effects are evaluated on the basis of [35], and the true density of the carbon-ash residue is determined in accordance with [36].

To evaluate the coefficients of convective mass and heat exchange between the active surface of a fuel particle and the surrounding gas we use the criterial dependences [21, 22] (see Table 1) allowing for the presence of inert ash particles in the bed. The coefficients of radiative heat exchange are found in accordance with the recommendations of [21].

A numerical analysis of the system of equations (1)–(14) is carried out on the basis of the iteration algorithm developed earlier [15, 16, 18, 19]. A distinguishing feature of the algorithm used in the present work is that the intermediate iterations for evaluation of the total rate of phase transition are eliminated from consideration; this makes the machine-calculation time much shorter and enables us to obtain an amount of numerical results larger than that in the equilibrium case and corresponding to the existing ideas of the physicochemical regularities of the processes of thermochemical processing of coals.

The calculation program for the process of thermocontact pyrolysis of a single particle of high-ash bituminous coal under nonequilibrium conditions is developed in the FORTRAN-90 language [37]. The initial data for calculations are the external operating conditions, the running size of coal and inert ash particles, and the physicochemical and structural characteristics of the fuel.

TABLE 1. Computational Formulas Used in Evaluating the Coefficients of Heat and Mass Exchange

Heat exchange	Mass exchange	Application conditions	Reference
$\mathrm{Nu} = \mathrm{Nu}_{\max} + (\mathrm{Nu}_1 - \mathrm{Nu}_{\max}) \times$ $\times \exp(-d_c/4d_a)$	$\mathrm{Sh} = d_a/d_c + 0.009\,\mathrm{Ar}_a^{0.5}[1 +$ $+ (30\,\mathrm{Ar}_a^{-1/6} - 1)]\exp(-d_c/d_a)$	$d_c \approx d_a = (10—60)$ mm $P_1 = 0.05—10$ MPa, $\mathrm{Ar}_a = 10^2—10^7$	[21]
$\mathrm{Nu}_{\max} = 0.85\,\mathrm{Ar}_a^{0.19} +$ $+ 0.006\,\mathrm{Ar}_a^{0.5}\,\mathrm{Pr}_1^{0.333}$		$d_c >> d_a$, $d_a = 0.13—2.15$ mm	[22]
$\mathrm{Nu}_1 = 10 + 0.23\,(\mathrm{Ar}_a\,\mathrm{Pr}_1)^{0.333}$		$\rho_a = 2300—3000$ kg/m^3, $\mathrm{Ar}_a = 40—10^5$ $d_c = 5.5—36.8$ mm	[22]
$\mathrm{Nu}_{a\infty} = 0.85\,\mathrm{Ar}_a^{0.19} +$ $+ 0.006\,\mathrm{Ar}_a^{0.5}\,\mathrm{Pr}_1^{0.333}$	$\mathrm{Sh}_{a\infty} = 0.009\,\mathrm{Ar}_a^{0.5}\,\mathrm{Sc}_1^{0.33}$	$\rho_a = 1150—2700$ kg/m^3 (heat exchange) $d_c = 2.4—21.9$ mm	
$\mathrm{Nu}_c = [(\mathrm{Nu}_1 — \mathrm{Nu}_{a\infty})\,(d_c/$ $d_a)^{1/3} + \mathrm{Nu}_{a\infty}(d_c/d_a)]\varphi^{2/3}$ (φ is the particle-shape factor)	$\mathrm{Sh}_c = (\mathrm{Sh}_1 — \mathrm{Sh}_{a\infty})\,(d_{c,p}/$ $d_{a,p})^{1/3} + \mathrm{Sh}_{a\infty}\,(d_c/d_a)$	$\rho_c = 820—2340$ kg/m^3 (mass exchange)	
$\mathrm{Nu}_1 = 6.0 + 0.117\,\mathrm{Ar}_a^{0.39}\,\mathrm{Pr}_1^{0.333}$	$\mathrm{Sh}_1 = 2\varepsilon_{mf} + 0.117\,\mathrm{Ar}_a^{0.39}\,\mathrm{Sc}_1^{0.333}$	$0.05 \le d_c \le 1.0$, $40 \le \mathrm{Ar}_a \le 10^7$	[22]
$N_{\mathrm{Sh}_c,\mathrm{Nu}_c} = 2 +$ $+ 0.6\,(\mathrm{Re}^{\mathrm{eff}})^{0.5}\,N_{\mathrm{Sc},\mathrm{Pr}_1}^{0.333}$		$d_c = d_a$	[22]
$\mathrm{Nu}_c = \mathrm{Nu}_1\,(d_c/d_a)^n$	$\mathrm{Sh}_c = \mathrm{Sh}_1\,(d_c/d_a)^m$	$d_c << d_a$, $1 \le d_c/d_a \le (d_c/d_a)_{cr}$, $n = 0.7$ $10 \le \mathrm{Ar}_a \le 10^5$, $n = 0.39\,\mathrm{Ar}_a^{0.105}$ $10^5 \le \mathrm{Ar}_a \le 10^7$, $\exp m = 0.58\,\mathrm{Ar}_c^{0.007}$ $10 \le \mathrm{Ar}_c \le 150$, $\exp m = 0.509\,\mathrm{Ar}_c^{0.1}$ $150 \le \mathrm{Ar}_c \le 10^7$, $(d_c/d_a)_{cr} = 5.35\mathrm{Ar}_a^{0.1}$ $10 \le \mathrm{Ar}_a \le 5 \cdot 10^4$, $(d_c/d_a)_{cr} = 2.8\mathrm{Ar}_c^{0.81}$ $5.0 \cdot 10^4 \le \mathrm{Ar}_c \le 3.0 \cdot 10^8$	[22]

The profiles of the variables (computed in all the phases in question) on the particle radius at different instants of time, the running size and degrees of conversion of the particle, the mean-integral yields of the *j*th component and the overall yields of pyrolysis products, the circumferential and radial thermal stresses developed in the particle, the reaction rate observed, the rates of heterogeneous chemical and phase transitions and those of primary release of volatiles and moisture, the effective coefficients of diffusion in the gas and intermediate condensed phases, the porosity of the particle and the volume fraction of the solid phase, and the apparent and true densities of the condensed and gas phases are results of the numerical analysis.

The calculations are completed once the total devolatization of the pores, a 90% overall yield of pyrolysis products, and a 95% degree of conversion of the fuel (or 0.1 of the initial particle radius) have been attained.

In numerical calculations, we have investigated the influence of the running size of the coal and inert ash particles, pressures, initial temperatures of the gas, the fuel, and the ash, coefficients of heat and mass exchange between the active particle surface and the surrounding gas, particle porosity, coefficients of capillary soaking and permeability, and different dependences for description of the primary release of volatiles on the course of the process of thermocontact pyrolysis of a single particle of GSSh (gas-flame seed stub)-grade high-ash bituminous coal. The parameters of the model were varied within the operating conditions of a TsKS-1.0 pilot demonstration technological unit [1–3, 20] developed at the Institute of Coal Power Technologies of the National Academy of Sciences and the Ministry of Fuel and Power of Ukraine for two-stage thermochemical processing (pyrolysis, burning, and gasification) of high-ash power-generating coal at pressures to 2.5 MPa and a high degree of circulation of the carbon-ash fuel residue (up to 100). One basic apparatus of this unit is the external pyrolysis apparatus with a lowering dense granular fuel bed; the pyrolysis apparatus in which thermocontact (due to the heating by ash particles) pyrolysis of the fuel fed to the unit

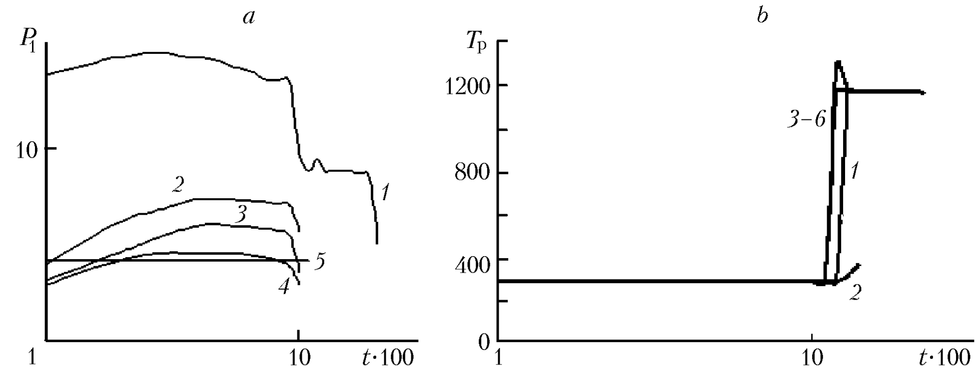

Fig. 1. Dynamics of change in the pressure (a) and the temperature (b) at the center of a GSSh-coal particle of diameter 1.0 mm with time for different values of the external pressure in calculations from the equilibrium model [18, 19]: 1) $P_1^0 = 0.1$, 2) 0.25, 3) 0.55, 4) 0.868, 5) 1.65, and 6) 2.5 MPa. P_1, Pa; t, sec; T_p, K.

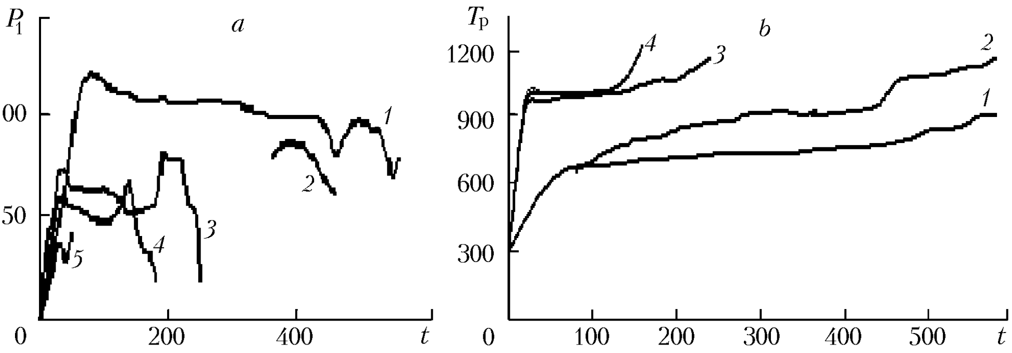

Fig. 2. Dynamics of change in the pressure (a) and the temperature (b) at the center of a GSSh-coal particle of diameter 1.0 mm with time and external pressure in calculations from the nonequilibrium model: 1) $P_1^0 = 0.25$, 2) 0.55, 3) 0.868, 4) 1.65, and 5) 2.5 MPa. P_1, Pa; t, sec; T_p, K.

is carried out under the conditions of high-rate heating and elevated pressures is located on the path of return of the carbon-ash fuel residue after the hot cyclone separator.

The calculation results have shown that the nonequilibrium model and the computational algorithm and program are quite efficient and stable, just as in the previous case [15, 16, 18, 19]; they enable us to obtain numerical results consistent with the existing ideas of the physicochemical regularities of the processes of processing of solid fuels and to attain, during the analysis, effective times and specific volatile yields comparable to those observed in pilot-scale and pilot-scale production units with a circulating fluidized bed that contains external pyrolysis apparatuses [1–3, 20]. (We made a comparative analysis of the calculation results in equilibrium and nonequilibrium formulations.)

The influence of the external pressure on the dynamics of change in the pressure and temperature at the center of a GSSh-coal particle in equilibrium and nonequilibrium formulations is shown in Figs. 1 and 2. It is seen that the character of change in the pressure is nearly analogous in both cases. The change in the pressure is the most intense in the initial stages of the process. The maximum value of pressure decreases in both the equilibrium (Fig. 1a) and nonequilibrium (Fig. 2a) cases; it is attained at large values of time. The increase in the pressure at the center of the particle in the initial stages is due to the intense evaporation of primary moisture and to the accumulation, in the pores, of the H_2O vapor displacing the remaining components from the particle. Further reduction in the pressure in the pores with increase in P_1^0 is related to the decrease in the gradients of this characteristic and accordingly in the rates of their convective-filtration transfer.

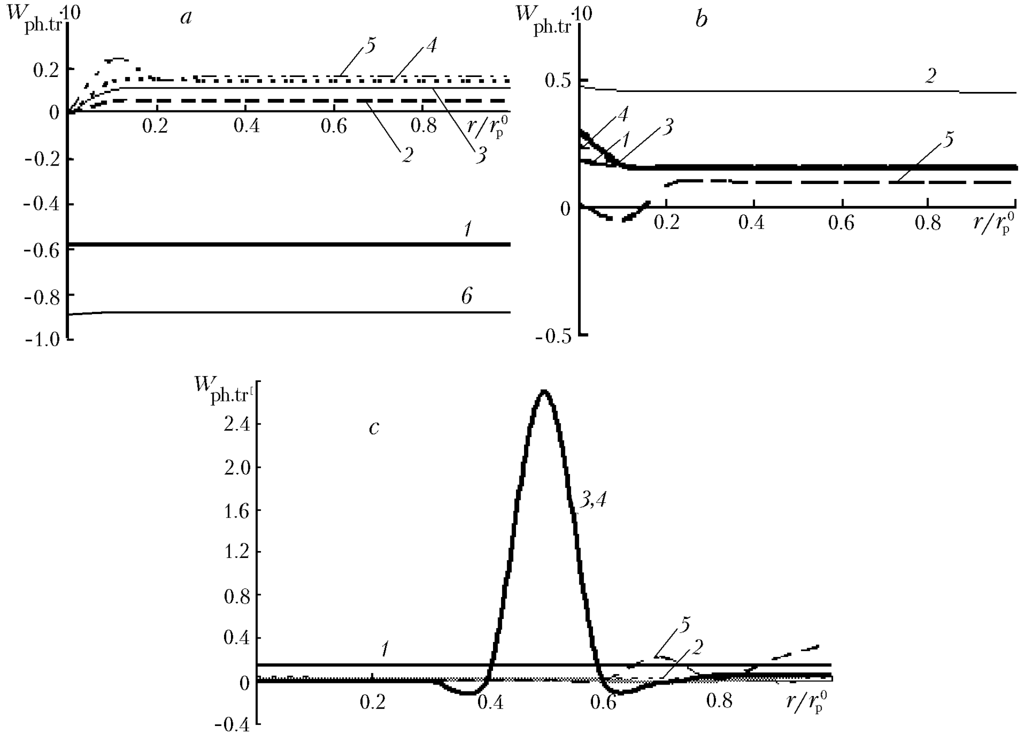

Fig. 3. Profiles of the phase-transition rates in calculations from the equilibrium model [18, 19]: a) $P_1^0 = 0.1$ MPa; 1) $t = 0.243$, 2) 0.124, 3) 0.0819, 4)0.0409, 5) 0.0205, and 6) 0.244 sec; b) $P_1^0 = 0.55$ MPa; 1) $t = 0.5\cdot 10^{-5}$, 2) $0.2\cdot 10^{-4}$, 3) $0.16\cdot 10^{-3}$, 4) 0.215, and 5) 0.232 sec; c) $P_1^0 = 0.868$ MPa (notation 1–5 is the same as in Fig. 3b). $W_{\rm ph.tr}$, kg/(m^3·sec).

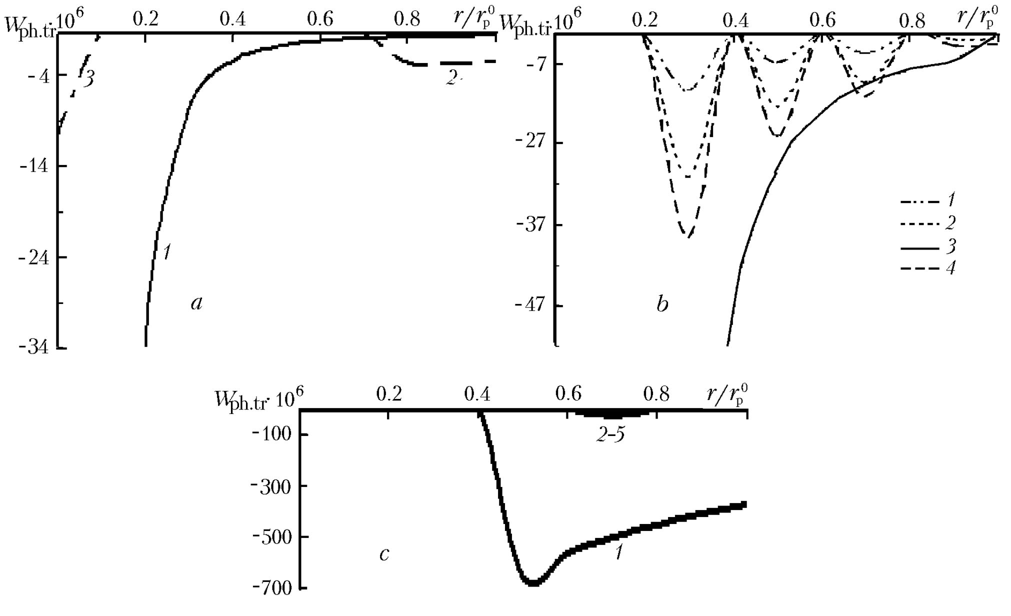

Fig. 4. Profiles of the phase-transition rates in calculations from the nonequilibrium model at $P_1^0 = 0.1$ (a), 0.55 (b), and 2.5 MPa (c): a) 1) $t = 0.1\cdot 10^{-4}$, 2) $0.825\cdot 10^{-2}$, 3) 0.0176, and 4) 0.068 sec; b) 1) $t = 0.225\cdot 10^{-4}$, 2) $0.154\cdot 10^{-1}$, 3) 0.138, and 4) 24.0 sec; c) 1) $t = 0.25\cdot 10^{-4}$, 2) $0.159\cdot 10^{-1}$, 3) $0.319\cdot 10^{-1}$, 4) $0.479\cdot 10^{-1}$, and 5) $0.63\cdot 10^{-1}$ sec. $W_{\rm ph.tr}$, kg/(m^3·sec).

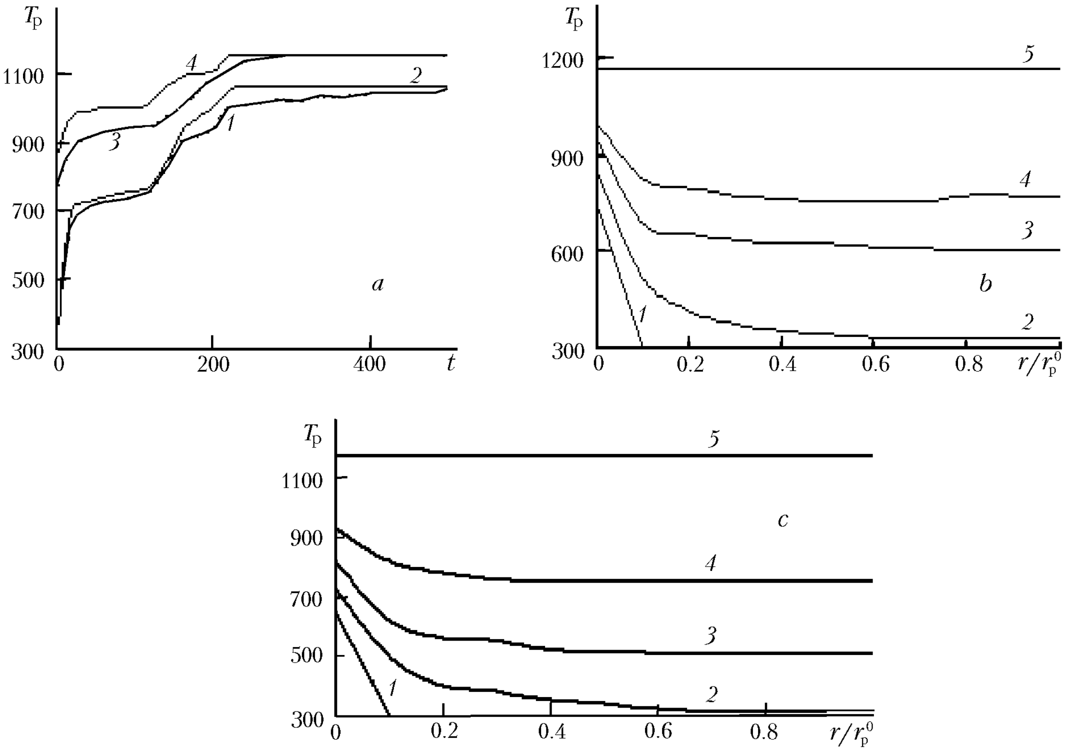

Fig. 5. Influence of the correlation dependences taken for evaluation of the coefficients of heat and mass exchange on the change in the particle temperatures in calculations from the nonequilibrium model: a) dynamics of change in the temperature of the center (1 and 3) and surface (2 and 4) of a GSSh-coal particle at $P_1^0 = 0.868$ MPa: 1 and 2) from [22] and 3 and 4) from [21]; b) temperature profiles on the particle radius for $P_1^0 = 0.868$ MPa in calculating the coefficients of heat and mass exchange from the correlations of [21]: 1) $t = 0.101$, 2) 1.74, 3) 11.3, 4) 101.6, and 5) 879.9 sec; c) the same, from the correlations of [22]: 1) $t = 0.1$, 2) 1.3, 3) 20.0, 4) 101.0, and 5) 561.9 sec. T_p, K; t, sec.

The character of change in the temperature at the center of the particle with external pressure is shown in Figs. 1b and 2b. Under equilibrium conditions, a sharp rise in the temperature at certain instants of time occurs due to the intense phase transitions of the components of resin and to the beginning of the processes proper of pyrolysis of the fuel and displacement of the gaseous products toward the exterior surface (Fig. 1b). Under nonequilibrium conditions, the particle temperature changes more smoothly and increases with external pressure (Fig. 2b). The characteristic pyrolysis times in the nonequilibrium process are longer than those in the equilibrium one.

The calculation results on comparison of the profiles of the phase-transition rates at different pressures under equilibrium and nonequilibrium conditions are presented in Fig. 3 and 4. In both cases we note a growth in the total rate of phase transition with pressure but in the first case the presence of both the evaporation and condensation zones in the pores is possible, whereas in the second case only the evaporation zone can be present.

No substantial influence of the dependences taken for evaluation of the coefficient of heat and mass exchange on the course of the process has been noted in calculations. The calculation results on the influence of the criterial formulas [21, 22] on the dynamics of change in the temperatures of the center and surface of a single GSSh-coal particle at $P_1^0 = 0.868$ MPa show that the given dependences (Fig. 5a) are fairly close in the case of thermocontact pyrolysis of coal-derived fuels. This is also demonstrated by the particle-temperature profiles given in Fig 5b and c. Also, the basic temperature gradients during the process are seen near the exterior particle surface in the stages of primary moisture and volatile release.

CONCLUSIONS

1. We have created a mathematical model, the algorithm, and the program for numerical analysis of the process of thermocontact pyrolysis of a single porous particle of high-ash power-generating coal under the operating conditions of technological units with a circulating fluidized bed under pressure. The effective diffusion, heat conduction, convective-filtration transfer, phase transitions and heterogeneous chemical transformations of pyrolysis products in the pores, stages of primary moisture and volatile release, convective heat and mass exchange, and radiative heat exchange between the active particle surface and the gas blanket with allowance for the presence of the inert ash particles in the bed have been taken into account. The case where the phase transitions of the pyrolysis products in the pores occur under nonequilibrium conditions has been considered.

2. The complex of numerical calculations of the influence of the model's parameters on the course of the process in the range required for ensuring the operating conditions of a pilot demo unit with a circulating fluidized bed under pressure has been performed.

3. It has been shown that the use of the nonequilibrium model makes it possible to substantially reduce the machine-computation time and to ensure a larger amount of numerical results than the equilibrium model. The results obtained are qualitatively consistent with the existing ideas of the physicochemical regularities of the processes of thermochemical processing of solid fuels.

NOTATION

$\mathrm{Ar} = [g(\bar{d}_{\mathrm{sort}})^3(\rho_i - \rho_1^0)]/(\rho_1^0\eta_1^2)$, Archimedes number; $b_0 \approx \tau k_0 \approx 2.0 - 3.6$ for the empirical coefficient $k_0 \approx 1.67 - 3.0$ and a coefficient of crookedness τ of the pores of 1.2 [24, 27, 34]; c_p, specific heat of the phase or the component at constant pressure, J/(kg·K); $c_{p1}^{\mathrm{eff}} = [c_{p1}\varepsilon_{\mathrm{mf}}\rho_1 + c_{p2}(1 - \varepsilon_{\mathrm{mf}})\rho_{\mathrm{a}}]/[\varepsilon_{\mathrm{mf}}\rho_1 + (1 - \varepsilon_{\mathrm{mf}})\rho_{\mathrm{a}}]$, effective heat capacity of the surrounding gas; C, concentration, weight fractions; D, diffusion coefficient, m^2/sec; d, diameter, m; E, activation energy, J/mole; F, specific surface, m^2/m^3; f, pore-size-distribution function; g, free fall acceleration, m/sec^2; H^*, coefficient of convective heat exchange, W/(m^2·K); k, rate constant at reference temperature, MPa^{-1}; L, total number of flooded pores; M, molecular weight, kg/kmole; $\underline{m}$, total number of components; N, total number of reactions; n, order of moisture and volatile release; $\mathrm{Nu} = H_{\mathrm{conv}}^* d_{\mathrm{c}}/\lambda_1^{\mathrm{eff}}$, effective Nusselt number; P, pressure, Pa; p, partial pressures of the reagents, MPa; $\mathrm{Pr}_1 = c_{p1}^{\mathrm{eff}}\mu_1/\lambda_1^{\mathrm{eff}}$, Prandtl number; Q, thermal effect of the reaction, J/mole; $\bar{q}$, rate of primary release of moisture and volatiles in the pores, kg/(m^3·sec); R, universal gas constant, J/(mole·K); r, radial coordinate of a particle, m; $\mathrm{Re}^{\mathrm{eff}} = \mathrm{Ar}_{\mathrm{c}}/[18 + 0.61\ (\mathrm{Ar}_{\mathrm{c}})^{0.5}] = \mathrm{Ar}_{\mathrm{a}}(d_{\mathrm{c}}/d_{\mathrm{a}})^3/\left\{18 + 0.61[\mathrm{Ar}_{\mathrm{a}}(d_{\mathrm{c}}/d_{\mathrm{a}})^3]^{0.5}\right\}$, effective Reynolds number [21]; $\mathrm{Re}_{\mathrm{cr}}^{\mathrm{eff}} = \mathrm{Re}_{\mathrm{mf}}/\varepsilon_{\mathrm{mf}} = \mathrm{Ar}_{\mathrm{a}}/[\varepsilon_{\mathrm{mf}}(1400 + 5.22(\mathrm{Ar}_{\mathrm{a}})^{0.5})]$, critical value of the Reynolds number beginning with which one can use the expression for $\mathrm{Re}^{\mathrm{eff}}$ [21, 22] (see Table 1); $\mathrm{Sc}_j = \eta_1/D_j^{\mathrm{m}}$, Schmidt number; $\mathrm{Sh}_j = \beta_j d_{\mathrm{c}}/D_j^{\mathrm{m}}$, Sherwood number; T, temperature, K; $T^* = T_1^0\varepsilon_{\mathrm{mf}} + T_{\mathrm{a}}^0(1 - \varepsilon_{\mathrm{mf}})$, effective temperature of the surrounding gas; t, time, sec; u, rate of convective-filtration transfer, m/sec; y, concentration, mole fractions; V, volume, m^3; W, reaction rate, kg/(m^3·sec); $\bar{W}$, total rate of phase transition in the pores, kg/(m^3·sec); W^{work} and V^{work}, initial fractions of moisture and volatiles in the fuel per working mass; α, volume fraction of the phase; B, capillary-soaking coefficient, m/sec; β, mass-exchange coefficient, m/sec; γ, permeability coefficient, m^3/(kg·sec); ΔH, heat of phase transition, J/kg; $\varepsilon_{\mathrm{c}}^*$, emissivity; ε, porosity; η, kinematic viscosity, m/sec; λ, thermal conductivity, W/(m·K); $\lambda_1^{\mathrm{eff}} = \lambda_1\varepsilon_{\mathrm{mf}} + (1 - \varepsilon_{\mathrm{mf}})\lambda_{\mathrm{a}}$, effective thermal conductivity of the surrounding gas; μ, coefficient of dynamic viscosity, Pa·sec; ν, stoichiometric coefficient; ρ, density, kg/m^3; σ_0, blackbody emission coefficient, W/(m^2·K^4); σ, surface tension, N/m; φ, wetting angle; $\bar{\Phi}$, sources of change in the concentrations in the solid phase, kg/(m^3·sec): $\bar{\Phi}_{\mathrm{c}} = \sum_{s=1}^{N_S} \nu_{sc} W_s \alpha_2 F_{\mathrm{sp}}$ for the coke, $\bar{\Phi}_{\mathrm{a}} = 0$ for the ash, $\bar{\Phi}_{\mathrm{vol}j} = \bar{q}_{\mathrm{vol}j}$ for the volatiles, and $\Phi_{\mathrm{w}} = \bar{q}_{\mathrm{w}}$ for moisture. Superscripts: eff, effective value; eq, equilibrium value; work, working mass; 0, initial value; *, effective value in the surrounding medium; $\bar{\ }$, averaging; m and res, molar and residual values. Subscripts: i, phase No.: 1, gaseous, 2, solid, 3, intermediate condensed; j, component No.: CO_2, 2, CO, 3, H_2O, 4, H_2, 5, CH_4, 6, C_2H_4, 7, C_2H_6, 8, C_6H_6, 9, C_7H_8, 10, $C_{11}H_{24}$, 11, $C_{12}H_{12}$, 12, $C_{13}H_{18}$, 13, $C_{14}H_{10}$, 14, C_6H_6O, 15, N_2; ph.tr, phase transition, vol, volatiles; w, moisture; s, No. of heterogeneous reaction; sol and liq, components of the solid and condensed phases; *l*, flooded pore; p, particle; 0, initial value; max, maximum; conv, convective; cap, capillary; min, minimum; mf, onset of fluidization; a, ash; cr, critical value; br, breakdown (critical) value of intraporous pressure at which the connectivity of phases is disturbed; gas, gaseous component; g, gas-filled pore; sort, sort of solid particles; c, coke (carbon); sp, specific.

REFERENCES

1. I. A. Vol'chin, Yu. P. Korchevoi, A. Yu. Maistrenko, et al., Burning of solid fuel in a pressurized fluidized bed, Preprint of the Scientific-Engineering Center of Coal Energy Technologies of the National Academy of Sciences and Ministry of Fuel and Energy of Ukraine, Kiev (1997).
2. A. Yu. Maistrenko, A. N. Dudnik, and S. V. Yatskevich, *Technology of Burning Coals for Steam-Gas Plants* [in Russian], Ukrainian Society "Znanie," Kiev (1993).
3. I. A. Vol'chin, N. V. Chernyavskii, G. N. Tal'nova, et al., *Production of Power and Domestic Gas by Means of Thermal Contact Pyrolysis in the PCC Loop*, Preprint of the Institute of Energy Saving Problems, National Academy of Sciences of Ukraine, Kiev (1993).
4. G. N. Makarov and G. D. Kharlampovich (Eds.), *Chemical Technology of Combustible Resources* [in Russian], Khimiya, Moscow (1986).
5. P. R. Solomon, M. A. Serio, and P. A. Suuberg, Coal pyrolysis: Kinetic rate and mechanisms, *Progr. Energy Combust. Sci.*, **18**, No. 2, 133–220 (1992).
6. V. G. Kashirskii, V. I. Bykov, and N. M. Tsyryul'nichenko, Kinetics of the process of thermal decomposition of fuel under the conditions of high-rate heating, in: *Collection of Scientific Papers "Complex Processing of Kansk-Achinsk Coals. Problems of Production of Synthetic Fuels* [in Russian], Izd. KrGU, Krasnoyarsk (1983), pp. 32–35.
7. B. A. Adenasya and Phan Hod Hun, Mathematical modelling of devolatization of coal particles in a convective environment, *Fuel*, **14**, No. 6, 896–904 (1995).
8. V. I. Bykov, T. I. Vishnevskaya, N. M. Tsyryul'nichenko, et al., Modeling of the dynamics of gasification of solid fuel particles, *Khim. Promyshlennost'*, No. 1, 58–60 (1995).
9. V. I. Bykov, T. I. Vishnevskaya, and N. M. Tsyryul'nichenko, Diffusional-kinetic model of combustion of coal particles in a gas flow, *Fiz. Goreniya Vzryva*, **33**, No. 4, 39–45 (1997).
10. G. A. Gerasimov, Modeling of the pyrolysis process of coal particles, *Inzh.-Fiz. Zh.*, **72**, No. 2, 253–259 (1999).
11. V. P. Patskov, A. A. Anishchenko, V. V. Kulichenko, et al., Mathematical simulation and calculation of the processes of thermochemical processing of single coal particles at elevated pressures, *Khim. Promyshlennost'*, No. 4, 253–259 (1995).
12. V. P. Patskov, V. V. Kulichenko, and T. V. Patskova, Numerical simulation of the processes of thermochemical conversion of single coal particles at elevated pressures, in: *Intrachamber Processes. Combustion and Gas Dynamics of Disperse Systems. 1st Int. School-Seminar* [in Russian], BGTU "Voenmekh" im. D. F. Ustinova, St. Petersburg (1995), pp. 152–154.
13. Yu. P. Korchevoi, V. P. Patskov, A. Yu. Maistrenko, and V. V. Kulichenko, Numerical simulation of processes of thermochemical transformation of single coal particles at elevated pressures, *Inzh.-Fiz. Zh.*, **69**, No. 6, 1000–1005 (1996).
14. S. G. Dulienko, N. V. Chernyavskii, G. N. Tal'nova, et al., Kinetics and mechanism of gas emanation in thermocontact pyrolysis of gas coal in a pressurized fluidized bed, in: *XI Symposium on Combustion and Explosion "Chemical Physics of the Processes of Combustion and Explosion"* [in Russian], Vol. 1, Pt. 1, Chernogolovka (1996), pp. 22–24.
15. L. S. Gaponich, I. G. Grin', G. N. Tal'nova, et al., Dynamics of gas emanation in thermocontact pyrolysis of Donetz gas coal in the reactor of thermocontact pyrolysis of the PCC gasifier, *Khim. Promyshlennost'*, No. 4, 9–13 (1995).
16. L. S. Gaponich, G. N. Tal'nova, and N. V. Chernyavskii, Gas emanation in thermocontact pyrolysis depending on pressure and medium, *Ékotekhnologii Resursosberezhenie*, No. 2, 13–17 (1998).

17. R. A. Kalinenko, A. A. Levitskii, L. S. Polak, et al., Computational-theoretical investigation of the process of pyrolysis and hydropyrolysis of coal, *Kinet. Katal.*, **26**, Issue 6, 1336–1343 (1985).
18. V. P. Patskov, Numerical analysis of the process of thermal decomposition of high-ash bituminous coal under the conditions of operation of circulating-fluidized-bed plants, *Dokl. Nats. Akad. Nauk Ukrainy*, No. 4, 100–108 (2001).
19. V. P. Patskov, Numerical analysis of the process of thermal decomposition of pressurized single particles of high-ash bituminous coal, in: *Proc. IV Minsk Int. Forum "Heat and Mass Transfer–MIF-2004"* [in Russian], Vol. 4, May 22–26, 2000, Minsk (2000), pp. 57–63.
20. Yu. P. Korchevoi, A. Yu. Maistrenko, and A. I. Topal, *Environmentally Pure Coal Technologies* [in Russian], Naukova Dumka, Kiev (2004).
21. I. P. Mukhlenov, B. S. Sazhin, and V. F. Frolov (Eds.), *Calculations of Fluidized-Bed Apparatuses: Handbook* [in Russian], Khimiya, Leningrad (1986).
22. G. I. Pal'chenok, G. G. Vasil'ev, A. F. Dolidovich, et al., Heat- and mass-transfer coefficients of an active particle freely moving in the fluidized bed of an inert disperse material, in: *Proc. 2nd Minsk Int. Forum "Heat and Mass Transfer–MIF-92"* [in Russian], Vol. 5, May 20–24, 1992, Minsk (1992), pp. 172–175.
23. V. P. Patskov, *Influence of Transfer Phenomena and Phase Transitions on the Macrokinetics of Gas-Liquid Heterogeneously Catalytic Processes*, Candidate's Dissertation (in Engineering), Novosibirsk (1988).
24. A. V. Luikov, *Heat- and Mass Transfer: Handbook* [in Russian], Énergiya, Moscow (1978).
25. V. A. Kirillov, *Reactors with Participation of a Gas, a Liquid, and a Solid Catalyst* [in Russian], Izd. SO Ross. Akad. Nauk, Novosibirsk (1997).
26. R. C. Reid, J. Prausnitz, and T. K. Sherwood, *The Properties of Gases and Liquids* [Russian translation], Khimiya, Leningrad (1991).
27. V. A. Kirillov, I. A. Mikhailova, and S. A. Fadeev, Investigation of critical phenomena in the course of exothermic reactions on a partially wetted porous grain of a catalyst, *Fiz. Goreniya Vzryva*, **38**, No. 2, 22–32 (2002).
28. O. Yu. Maistrenko, *Basic Laws Governing the Combustion and Gasification of Coal in Different Modifications of a Fluidized Bed*, Candidate's Dissertation (in Engineering), Institute of Gas, National Academy of Sciences of Ukraine, Kiev (1999).
29. L. D. Smoot and D. T. Pratt (Eds.), *Pulverized Coal Combustion and Gasification: Theory and Applications for Continuous Flows Processes*, Plenum Press, New York and London (1978).
30. B. P. Nikol'skii, V. N. Grigorov, B. E. Pozin, et al., *Chemical Engineer's Handbook* [in Russian], Khimiya, Moscow (1963).
31. B. P. Nikol'skii (Ed.), *Physical Chemistry. Theoretical and Applied Manual: Textbook for Higher Educational Institutions* [in Russian], Khimiya, Leningrad (1987).
32. K. F. Pavlov, P. G. Romankov, and A. A. Noskov, *Examples and Problems in the Course "Processes and Apparatus of Chemical Technology"* [in Russian], Khimiya, Moscow (1981).
33. M. V. Boboshin, E. A. Krichevtsov, V. M. Abzamov, et al., *Thermophysical Properties of Fuels and Charge Materials of Ferrous Metallurgy* [in Russian], Metallurgiya, Moscow (1982).
34. O. A. Malinovskaya, V. S. Beskov, and M. G. Slin'ko, *Modeling of Catalytic Processes on Porous Grains* [in Russian], Nauka, Novosibirsk (1975).
35. S. D. Beskov, *Technochemical Calculations* [in Russian], Vysshaya Shkola, Minsk (1966).
36. V. N. Yurenev and D. P. Lebedev (Eds.), *Heat-Engineering Handbook* [in Russian], Énergiya, Moscow (1976).
37. M. Metcalf and J. Reed, *Programming Language FORTRAN-90* [Russian translation], Mir, Moscow (1995).